

APPLYING RECURRENCE PLOTS TO IDENTIFY BORDERS BETWEEN TWO-PHASE FLOW PATTERNS IN VERTICAL CIRCULAR MINI CHANNEL

Mariusz FASZCZEWSKI*, Grzegorz GÓRSKI*, Romuald MOSDORF*

*Faculty of Mechanical Engineering, Białystok University of Technology, ul. Wiejska 45 C, 15-351 Białystok, Poland

mariusz.faszczewski@gmail.com, grzesgor@o2.pl, mosdorf@gmail.com

Abstract: In the paper the method based on recurrence plots has been used for identification of two-phase flow in a vertical, circular mini-channel. The time series obtained from image analysis of high speed video have been used. The method proposed in the present study allows us to define the coefficients which characterize the dynamics of two-phase flow in a mini channel. To identify two-phase flow patterns in a mini channel there has been used the coefficient LAVG which is a measure of an average length of diagonal lines in recurrence plot. The following two-phase flow structures have been considered: bubbly, bubbly-slug and wavy-annular. Obtained results show that method proposed in the paper enables identification of borders between two two-phase flow patterns coexisting in a mini-channel.

Key words: Mini-Channel, Two-Phase Flow, the Method of Recurrence Plots, Nonlinear Analysis, Bubble Pump

1. INTRODUCTION

Numerous experimental studies carried out in recent years in many universities indicate that the two-phase flows in mini-channels are accompanied by fluid behaviors different from those observed in traditional channels (Zhao and Rezkallah, 1993). The flows in mini-channels should be considered taking into account such phenomena as surface tension, liquid pressure oscillation and the reverse flow (Wongwises and Pipathattakul, 2005).

Despite many experimental and theoretical researches, in the literature there is no clear classification of patterns of two-phase flow and types of channels (Chen et al., 2006). Therefore, it is difficult to compare the experimental results, especially when they are carried out for different fluids or different experimental conditions. It is believed that the criterion for distinguishing between types of channels should be based on the channel size and fluid properties (Chen et al., 2006). Usually, the criteria for distinguishing a mini-channel from the traditional channel are based on different numbers of similarities.

Kew and Cornwell proposed the criterion of $Co > 0.5$ (Kew and Cornwell, 1997). Brauner and Moalem-Maron proposed criterion based on the dimensionless numbers of EO . They suggest that when the $EO > 1$, then the surface tension plays an important role in the flow (Brauner and Moal-Maron, 1992). Triplett et. al proposed a criterion in the form of: $EO = 100$ (Triplett et al, 1999). Abkar proposed the criterion in the form of $Bo = 0.3$. The above criteria determine different critical channel diameters which define mini-channels. For air and water channel the critical diameter based on above criterions are in the range from 0.81 to 17.1 mm (Abkar et al., 2003). In the present study the two-phase flow in a vertical, circular channel with a diameter of 4 mm has been analyzed.

Identification of flow patterns in mini-channels often depends on subjective evaluation of the observer and used experimental technique. The flow patterns can change rapidly but usually this change happens slowly and the border between different patterns

is clear. Because of this, the significant scatter in results presented by different researches are observed (Kandlikav, 2002). For parameters characterizing the transition between patterns the two phase flow is usually unsteady. In such situation, the criteria based on average values of the various parameters are not suitable to identify the border between flow patterns. Therefore, the new criterion based on properties of dynamics of two phase flow is required.

In the present paper the method of analysis of video recorded using a high-speed camera has been presented. This method allows us to determine the coefficients characterizing the dynamics of two-phase flows. The recurrence plot method has been used. This method allows us to analyze the dynamics of nonlinear systems with large numbers of freedom degrees. The proposed method was applied to analyze two-phase flows in bubble pump (Benhmidene et al., 2010).

2. METHODS OF EVALUATION OF TWO-PHASE FLOW DYNAMICS

The scheme of experimental stand is shown in Fig.1.

The compressed air generated by the compressor (13), is passing through the tank (12), valve (11), rotameter (10) and a brass nozzle with an inner diameter of 1.1 mm. Air bubbles rising on the nozzle outlet moving in a glass mini-channel (2) with internal diameter of 4 mm and a length of 45 mm, is placed in a glass tank (1) of 400 x 400 x 700 mm filled with distilled water. The movement of air bubbles was recorded by the camera (3) with speed 600 frames/s. Examples of images recorded during the experiment are shown in Fig. 2a. In Fig. 2a the schematic drawing of the flow patterns in mini-channel has been presented.

In the mini-channel the following flow patterns are observed: bubbly, bubbly-slug and wavy-annular. For the flow rate $q < 0.05$ l/min, single bubbles with diameters equal to channel diameter have been observed. In the range of $0.05 < q < 0.1$ l/min the flow with long bubbles (Taylor) occurs. In this case a slight variation

of its length and spacing between them was observed (no-observed merger of bubbles). For $q = 0.2$ l/min the process of grouping bubbles in groups of two, three or more bubbles appears. But usually, the line between aggregated bubbles is visible. For $q = 0.3$ l/min bubbles coalesce and form the long slugs, in which the individual bubbles are indistinguishable. The wave-annual flow is formed at $q = 0.4$ l/min.

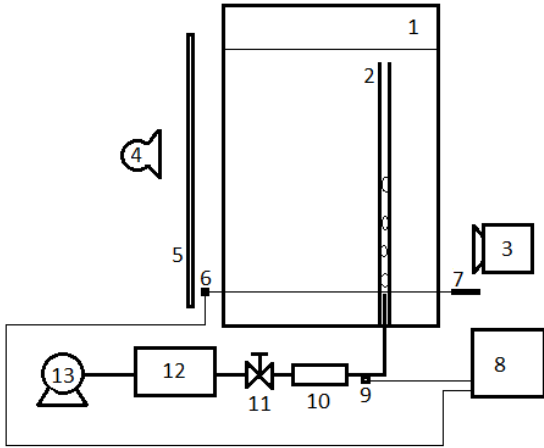


Fig. 1. Scheme of experimental stand: 1 – the water tank, 2 – mini-channel, 3 – Camera Casio EX FX1, 4 – light source, 5 – screen, 6 – phototransistor, 7 – laser, 8 – data acquisition station (DT9800) 9 – pressure sensor (MPX12DP), 10 – rotameter (Kytola OY, A-2k), 11 – valve, 12 – tank of air, 13 – air compressor

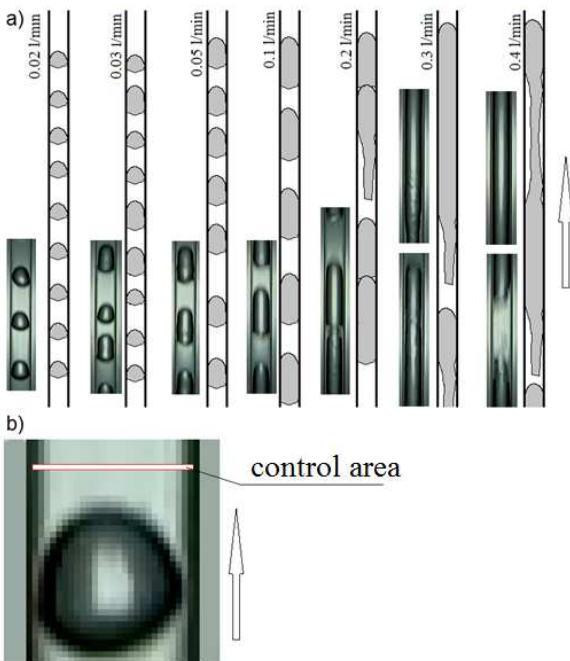


Fig. 2. The flow patterns in mini-channel as a function of air volume flow rate (a). The example of video frame with a selected area in which the brightness of pixels has been counted (b)

The film made for high speed digital camera (600 frames/s) has been divided into separated color frames. An example of a video frame is shown in Fig.2b. Then, the location of the control area has been determined. In the control area the sum of pixels brightness in each frame has been calculated. The ex-

ample of control area location is shown in Fig.2b. The actual size of the control area is: 0.16 x 4 mm.

Each pixel is characterized by three values of the colour component (RGB). The average brightness of each pixel has been calculated and then, in the control area all brightness values have been summed, according to the relation.

$$x_t = \sum_i \left(\frac{x_R^i + x_G^i + x_B^i}{3} \right)_t \quad (1)$$

where: i – the number of pixels in the control area, t – number of video frames.

Finally, the time series characterizing the two-phase flow in mini-channel have been obtained. The example of series obtained at different air volume flow rate has been shown in Fig. 3. High values in time series correspond to situations where the control area is filled with water. Low values correspond to situation where the control area is filled with air. In the centre of the air bubble the pixels brightness is low, therefore, in time series the values of x_i are not constant when the bubble passes through the control area. But the beginning and the end of bubble is clearly identified in time series x_i .

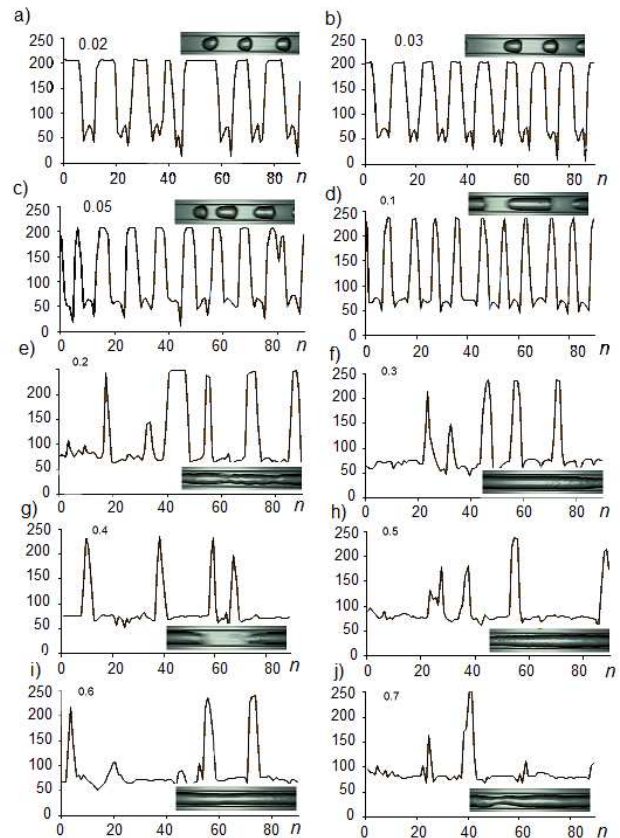


Fig. 3. Time series obtained from the films made by the high speed digital camera as a function of air volume flow rates. a) $q = 0.02$ l/min, b) $q = 0.03$ l/min, c) $q = 0.05$ l/min, d) $q = 0.1$ l/min, e) $q = 0.2$ l/min, f) $q = 0.3$ l/min, g) $q = 0.4$ l/min, h) $q = 0.5$ l/min, i) $q = 0.6$ l/min, j) $q = 0.7$ l/min

3. DATA ANALYSIS

Identification of the behaviour of dynamic systems based on experimental data proceeds in several steps. The analysis

begins from the reconstruction of the attractor, which is performed in the embedding space, using the so-called time delay method (Schuster, 1993). In this method the coordinates of attractor points are calculated from time series as successive values of time series. The distance between these values (delay time) is equal to τ . The time delay τ is a multiple of time interval Δt between points of time series (Baker and Gollub, 1998). The selection of the appropriate time delay has a significant impact on the reconstruction. There are many methods of determining the optimal values of the time delay. One of them is based on analysis of the autocorrelation function. The optimal value of the time delay is calculated as follows (Baker and Gollub, 1998):

$$C(\tau) \approx \frac{1}{2} C(0) \quad (2)$$

where: $C(\tau) = \frac{1}{N} \sum_i (x_i - x_{i+\tau})^2$

Fig. 4 shows the 3D reconstruction of the attractor obtained for the time delay obtained from equation (2).

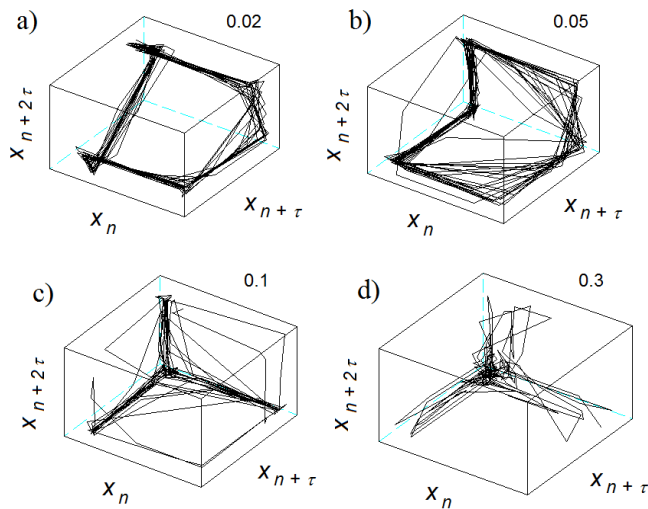


Fig. 4. 3D reconstruction of the attractors for time series shown in Fig. 3. a) $q = 0.02$ l/min, $\tau = 4$. b) $q = 0.05$ l/min, $\tau = 3$. c) $q = 0.1$ l/min, $\tau = 2$. d) $q = 0.3$ l/min, $\tau = 5$

The values of investigated time series oscillate between two levels. The high level represents the case when the control region (Fig. 2b) is filled with water. Brightness oscillations in this case are small. The low level occurs when in the control area the air bubble occurs. In this case, there are oscillations of brightness due to the changes of the bubble shape. Time intervals in which time series values have small changes (low or high signal level) create these parts of attractor in which the trajectories concentrate. For small q the concentration of trajectories is caused by low and high values of the series (Fig. 4). At high values of q only the low values of time series are responsible for trajectories concentration (Fig. 4d).

The correct embedding dimension in which the attractor should be reconstructed is determined by the correlation dimension. For the experimental data the correlation dimension D_2 can be determined by the following formula (Parker and Chua, 1987; Grassberger and Procacci, 1983):

$$D_2 = \lim_{l \rightarrow 0} \frac{1}{l} \ln \sum_i p_i^2 \quad (3)$$

where: $\sum_i p_i^2 \approx \lim_{N \rightarrow \infty} \frac{1}{N^2} \sum_{i,j} \theta(r - |x_i - x_j|) = C_2(r)$, θ – Heaviside step function.

The quantity C_2 , called the correlation integral, determines the probability of finding in the attractor the two points with distance less than r . In order to determine the correlation dimension, the slope of the regression line in linear part of the log plot $\log[C(r)] - \log(r)$ is calculated. Correlation dimension of attractors obtained from recorded time series as a function of air volume flow is shown in Fig. 5.

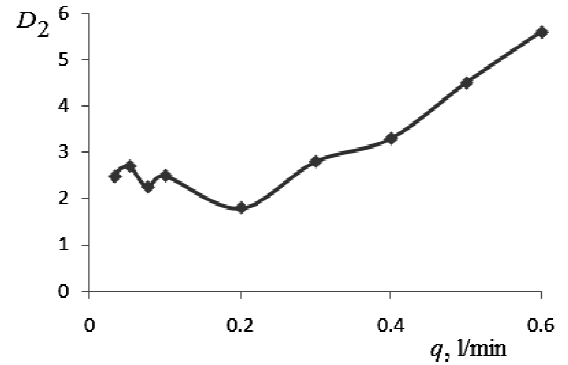


Fig.5. Correlation dimension (D_2) of recorded time series vs air volume flow rate

The recurrence plot (RP) is used to evaluate the degree aperiodicity of nonlinear systems. It is also helpful in the analysis of the attractor reconstructed in multidimensional phase space. The recurrence plot is always two-dimensional even though it may represent the system behaviours in the multi-dimensional space. The recurrence plot is described by the relation (Marwan et al., 2007):

$$R_{i,j} = \theta(\varepsilon_i - \|x_i - x_j\|) \quad (4)$$

where $i, j = 1 \dots N$, N number of considered points x_i , ε_i the search radius, $\| \cdot \|$ norm, θ Heaviside step function.

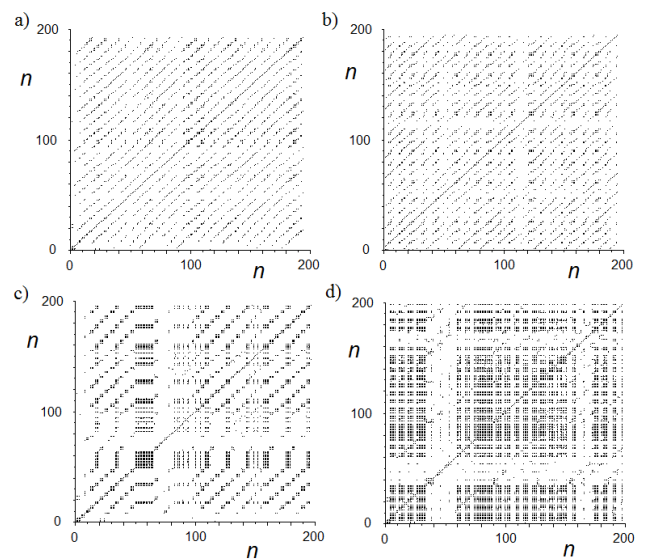


Fig. 6. Recurrence plots (RP) obtained for time series shown in Fig. 3., ε_i are equal to 10% of the maximum attractor diameter a) $q = 0.02$ l/min, $\tau = 4$. b) $q = 0.05$ l/min, $\tau = 3$. c) $q = 0.1$ l/min, $\tau = 2$. d) $q = 0.3$ l/min, $\tau = 5$.

The recurrence plot is defined for attractor immersed in spaces which dimension is the smallest integer number greater than the correlation dimension of attractor. For the air volume flow rate $q \leq 0.3$ l/min the proper embedding dimension is equal to 3. For the larger air volume flow rate the embedding dimension is respectively equal to 4, 5 and 6 (Fig. 5). In Fig. 6 it has been shown the recurrence plots for selected air volume flow rates. For all recurrence plot there has been assumed that threshold ϵ_i is equal to 10% of the maximum attractor diameter.

Analysis of the shape of the attractor created from measurement data shows that one of characteristic feature of attractor is the area where the attractor trajectories are concentrated. The length of the slug and distance between successive slugs decide on the size of this area. On the other hand, the appearance of those areas is determined by states in which the values of time series vary slightly. Attractor points located in the areas, where attractor trajectories are concentrated, form diagonal and vertical lines on the recurrence plot. The analysis of the length of diagonal lines is carried out, using the coefficient $LAVG$ and $ENTR$, whereas the length of the vertical line describes the coefficient TT .

The average length of diagonal lines, $LAVG$, is defined by the following relation (Marwan et al., 2007):

$$LAVG = \frac{\sum_{l=l_{min}}^N lP(l)}{\sum_{l=l_{min}}^N P(l)} \quad (5)$$

where $P(n)$ is the number of diagonal lines of length l .

The value of $LAVG$ is a measure of the average time, in which the two segments of the trajectories are close each other (Marwan et al., 2007). In Fig. 7 it has been shown the changes of function $LAVG$ vs air volume flow rate.

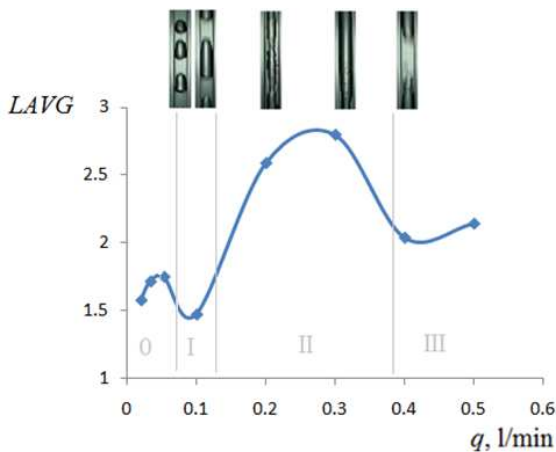


Fig. 7. Changes of $LAVG$ coefficient vs air volume flow rate

In Fig. 7 the range of changes q has been divided into four areas. The bubbly flow appears in the channel in the range marked with symbol "0". With the increase of air volume flow rate the bubble length increases. Such process causes increasing the number of attractor points created by point of time series with a low value. It causes the increase of value of coefficient $LAVG$. Further increase in air volume flow rate leads to decreases of gaps between the bubbles, which leads to decrease of the coefficient $LAVG$. Thus, in the range marked with symbol '0'

(Fig. 7) there is a maximum of function $LAVG(q)$. In this point, the dynamic equilibrium between two processes which determine the bubbly flow mini-channel (the growth of the length of the bubble and reducing the distance between the bubbles) appears.

In the range of q marked with symbol "I" the coefficient $LAVG$ decreases reaching a minimum at $q \sim 0.1$ l/min. The reduction of coefficient $LAVG$ is caused by oscillations of distance between successive bubbles. These oscillations lead to increase of distance between attractor trajectories (Fig.5c). Therefore, the obtained result allows us to divide the range marked with symbol "I" (slug flow) into two sub-ranges:

- in the first sub-range the oscillations of distance between slugs gradually increase. This process leads to drop in the value of the coefficient $LAVG$,
- in the second sub-range the length of slugs gradually increases. This process leads to increase of values of the coefficient $LAVG$.

The value of q for which the function $LAVG(q)$ reaches a minimum is a point of dynamic equilibrium between two processes which determine the slug flow in the mini-channel.

In the range "II" the function $LAVG(q)$ reaches a maximum. In the initial part of the range "II" bubble coalescence leads to the formation of long slugs. It causes to increase of the value of the coefficient $LAVG$. In the final phase of region "II" the long slugs are divided into smaller ones due to the flow instability. This process leads to decrease of the value of coefficient $LAVG$. The wave-annual flow is formed at $q = 0.4$ l/min. In this case, the average length of long slugs stabilizes causing small changes of $LAVG$ coefficient with increasing the air volume flow rate. The obtained result allows us to divide the area "II" into two sub-ranges:

- in the first sub-range the process of increasing the average length of joined slugs appears,
- in the second sub-range the average length of long slugs is reduced.

The maximum of function $LAVG(q)$ defines the point of dynamic equilibrium between those two processes.

The coefficient $ENTR$ determines the probability of finding the diagonal line of length l . Its value is related to the Shannon entropy. $ENTR$ is calculated by the following relation (Marwan et al., 2007):

$$ENTR = - \sum_{l=l_{min}}^N p(l) \ln p(l) \quad (6)$$

where the probability of finding a line of length is defined as follows (Marwan et al., 2007):

$$p(l) = \frac{P(l)}{\sum_{l=l_{min}}^N P(l)} \quad (7)$$

It is the ratio of the number of diagonal lines with length of l to the sum of all diagonal lines whose length is greater than l_{min} . Fig. 8 shows the changes of the function $ENTR(q)$ for l_{min} equal to 3.

The function $ENTR$ has two maxima and one minimum. The coefficient $ENTR$ increases together with increase of probability of existence of the line with the length greater than l_{min} in RP. It happens when average length of diagonal lines increases (for $q = 0.05$ l/min and $q = 0.3$ l/min, Fig. 7). Thus, the obtained result corresponds to result obtained for coefficient $LAVG$.

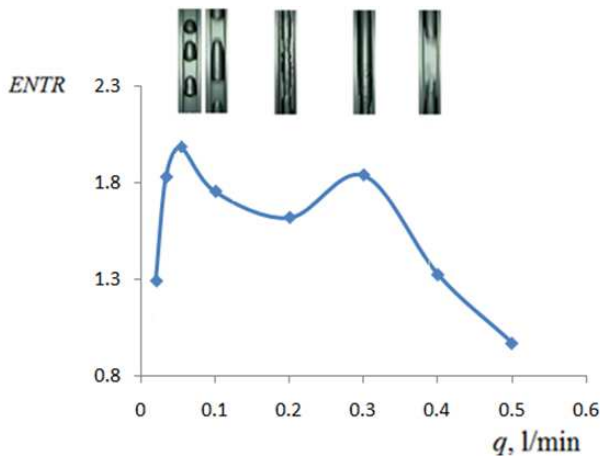


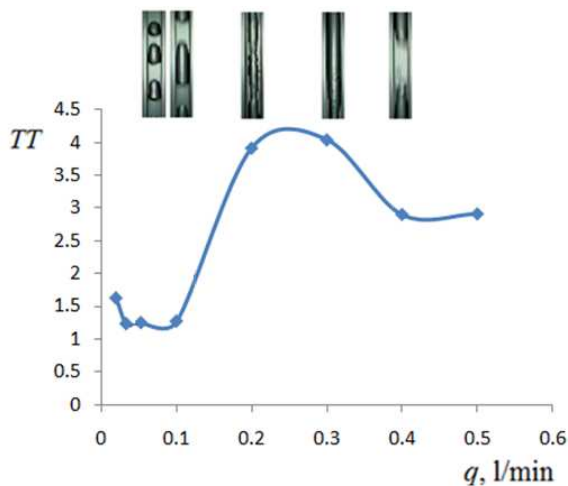
Fig. 8. Changes of coefficient ENTR vs air volume flow rate

The coefficient TT (trapping time) determines the average length of the vertical line and is described by the relation (Marwan et al., 2007):

$$TT = \frac{\sum_{v=v_{\min}}^N vP(v)}{\sum_{v=v_{\min}}^N P(v)} \quad (8)$$

where $P(v)$ is the number of vertical lines of length v .

The coefficient, TT , identifies the average length of the areas on RP, where the state of the system does not change. Fig. 9 shows the changes of TT as a function of air volume flow rate.



Rys. 9. Changes of the coefficient TT as a function of air volume flow rate

When a slug length is large, the results obtained using the coefficient TT are similar to results obtained using the coefficient $LAVG$. The difference occurs for small values of q for which there is a small number of vertical lines on the RP.

4. CONSLUIONS

In the paper, to identify the boundaries between two-phase flow patterns in mini-channel the three coefficients characterizing the structure of recurrence plot have been used:

- coefficient $LAVG$ is a measure of the average time in which the trajectories segments are close together;
- coefficient $ENTR$ is a measure of entropy of probability of finding the diagonal line of length greater than l_{min} on the RP;
- coefficient TT is the average length of the segment of attractor where the state of the system does not change. In this case a large slug passed through the control area.

Obtained results show that using RP allows us to identify borders between dynamically coexisting flow patterns in mini-channel. The coefficient $LAVG$ seems to be the most useful in order to identify the borders between different patterns of two-phase flows. Results presented in the paper should be treated as a preliminary once. It is necessary to conduct further research to identify the usefulness of RP for analysing the dynamics of two-phase patterns in mini-channel.

REFERENCES

1. Akbar M.K., Plummer D.A. and Ghiaasiaan S.M., (2003) On gas-liquid two-phase flow regimes in microchannels, *International Journal of Multiphase Flow*, Vol. 29, 855-865,
2. Baker G.L., Gollub J.P. (1998) *A Tutorial of dynamic of chaotic systems (in polish)*, Wydawnictwo Naukowe PWN, Warszawa
3. Benhmidene, A., B. Chaouachi and S. Gabsi, (2010). A review of bubble pump technologies. *J. Applied Sci.*, 10: 1806-1813.
4. Brauner N. and Moalem-Maron D., (1992) Identification of the range of small diameter conduits, regarding two-phase flow pattern transitions, *Int. Commun. Heat Mass Transfer*, Vol. 19, 29-39
5. Chen L., Tian Y.S. and Karayiannis T.G., (2006) The effect of tube diameter on vertical two-phase flow regimes in small tubes. *International Journal of Heat and Mass Transfer* 49, 2006, 4220-4230
6. Grassberger P., Procaccia I., (1983) Characterization of Strange Attractors, *Physical Review Letters* 505
7. Kandlikav S.G., Fundamental issues related to flow boiling in minichannels and microchannels, *Experimental thermal and Fluid Science*, Vol. 26, 389-407
8. Kew P.A. and Cornwell K., (1997) Correlations for the prediction of boiling heat transfer In small-diameter channel, *Applied Thermal Engineering*, Vol.17, No. 8-10, pp.705-715
9. Marwan, N.; Romano, M. C.; Thiel, M., Kurths, J. (2007). Recurrence Plots for the Analysis of Complex Systems, *Physics Reports*, 438(5-6), pp. 237-329. Recurrence Plots And Cross Recurrence Plots (www.recurrence-plot.tk)
10. Parker T. S, Chua L. O., (1987) A Tutorial for Engineers, *Proceedings of The IEEE*, vol. 75, No. 8,
11. Schuster H.G. (1993) *Chaos deterministyczny – wprowadzenie*, Wydawnictwo Naukowe PWN, Warszawa
12. Triplett K. A., Ghiaasiaan S.M., Abdel-Khalik S.I. and Sadowski D.L., (1999) Gas-liquid two-phase flow in microchannels, Part I: Two-phase flow patterns, *International Journal of Multiphase Flow*, Vol. 25., 377-394,
13. Wongwises S., Pipathattakul M. (2006) Flow pattern, pressure drop and void fraction of two-phase gas-liquid flow in an inclined narrow annular channel. *Experimental Thermal and Fluid Science*, 30 (2006) 345-354.
14. Zhao L., Rezkallah K.S., (1993) Gas-liquid flow patterns at micro-gravity condition, *International Journal Multiphase Flow* 19, 751-763.